Effect of Solvent Polarity on the Initiation and the Propagation of Ethylene Polymerization with Constrained Geometry Catalyst/MAO Catalytic System: A Density Functional Study with the Conductor-Like Screening Model

Sung Hoon Yang, June Huh, and Won Ho Jo*

Hyperstructured Organic Materials Research Center and School of Materials Science and Engineering, Seoul National University, Seoul 151-742, South Korea

Received September 2, 2004; Revised Manuscript Received December 1, 2004

ABSTRACT: The effect of solvent polarity on the initiation and propagation of ethylene polymerization with a constrained geometry catalyst (CGC) and MAO counterion was investigated by the density functional theory (DFT) with the conductor-like screening model (COSMO). Structures and energetics of reactant, π-complex, transition state, γ-agostic product, and β-agostic product during insertion of ethylene monomer into the catalytic active species of ionic pair or cationic catalyst are analyzed using the software DMol^3. A comparative analysis on the energetics of the ethylene insertion in the gas state and in solvents with different dielectric constants (ϵ) shows that the solvent polarity affects the energetics of monomer insertion very differently depending upon the model for active catalytic species and/or polymerization stage. This different behavior provides a very useful method for identifying the real active catalytic species in experiment. The two important features of molecular structure determining the dependency of enegetics on the solvent polarity are the degree of exposure of the Ti atom on the solvent medium and the degree of separation of ionic pair during monomer insertion.

I. Introduction

The metallocene catalysts have several desirable properties such as high activity, an ability to produce high-molecular-weight polymers with a narrow molecular-weight distribution and a potential for rigorous control of stereoselectivity by tailoring metallocene ligands.[1−4] Such fascinating properties of the metallocene catalyst have invited a large number of experimental[5−7] and theoretical[8−33] studies on the metallocene-based polymerization. Although those studies have contributed to understanding of the mechanism of monomer insertion into an active site of the catalytic species in the polymerization to some extent, the mechanism of monomer insertion has not been clearly understood, because the true active catalytic species in the polymerization has not been fully elucidated. For instance, the role of counterion during monomer insertion in the polymerization has been under debate until recently. The cationic model,[15,34−39] which has been a conventional model for theoretical study on the metallocene-based polymerization, is based on the assumption that an ionic pair of a cationic catalyst and a counterion is completely separated from each other during monomer insertion, and therefore, the model neglects the effect of the counterion on polymerization in the calculation of energetics. In contrast, the ionic pair (IP) model[40−53] assumes that the catalytic active species can be stabilized by the strong electrostatic attraction with its counterion, and therefore an approaching monomer intrudes into the ionic pair of the two ionic species.[54] Although the IP model seems to be more realistic for monomer insertion, the situation on the real active catalytic species becomes even more complicated when one considers the effect of solvent. For instance, some experimental studies suggest that the ionic pair may be separated from each other in the polymerization under polar solvent media.[55,56]

To date, however, the solvent effect on the monomer insertion mechanism has not been fully understood, despite some theoretical studies have been reported.[43,51,53,57] Recently, Lanza et al.[51] reported the solvent effect on polymerization using ab initio quantum mechanical calculation when ethylene is polymerized with a constrained geometry catalyst (CGC) in the presence of a boron-based cocatalyst. More specifically, they calculated the effect of solvent polarity on the energetics of ethylene insertion by assuming that the solvent is a continuum of uniform dielectric constant. However, their concern about the solvent effect is restricted only to the first ethylene insertion, i.e., the initiation of polymerization, and thus the solvent effect on propagation is not taken into account. More recently, Xu et al.[53] studied the second insertion of ethylene, i.e., the propagation of polymerization, while the solvent effect was incorporated into their calculation for the second ethylene insertion, by using the density functional theory (DFT) combined with molecular mechanics. However, their result cannot be generalized because they considered only one kind of solvent, cyclohexane, and also assumed the IP model for an active catalytic species in their calculation.

Our primary objective is to investigate the effect of solvent polarity on the ethylene polymerization using both the cationic and IP models. For this purpose, the structural and energetical characteristics of ethylene polymerization with CGC/MAO catalytic system are calculated using quantum mechanical calculations based on the DFT. The effect of solvent polarity is considered by treating the solvent as the continuum of uniform dielectric constant in the DFT calculation. For the

* To whom correspondence should be addressed. Telephone: +82-2-880-7192. Fax: +82-2-885-1748. E-mail: whjpoly@plaza.snu.ac.kr.

10.1021/ma0481961 CCC: $30.25
Published on Web 01/19/2005

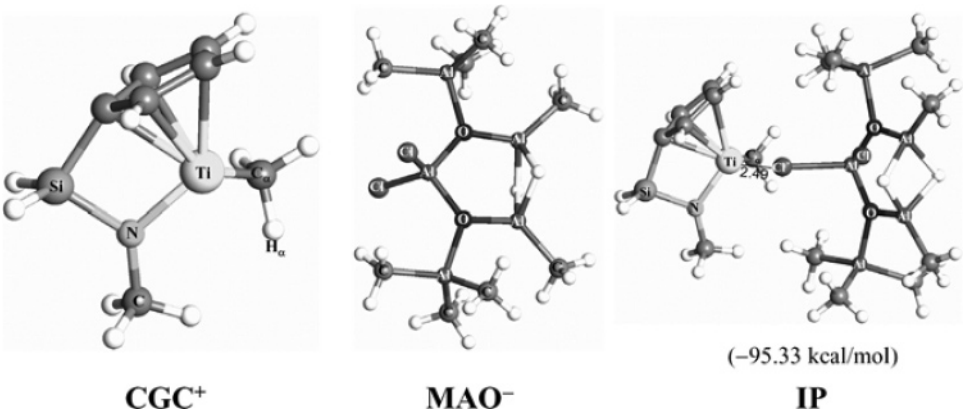

Figure 1. Optimized structure of the cationic catalyst (**CGC**$^+$), chlorinated MAO counterion (**MAO**$^-$) and ionic pair (**IP**) of the two ionic species. The energy saved from formation of an ionic pair (**IP**) of **CGC**$^+$ and **MAO**$^-$ is given in parentheses.

catalytic active species, both the cationic model and the IP model are considered and the results are compared to each other.

II. Computational Details

Fundamentals of the computational method are similar to those in our previous works[39,58] except for an additional incorporation of dielectric continuum into the calculation in order to take the solvent effect into account. All calculations were performed using the DMol^3 program (Accelys Inc.) based on DFT.[59] An accuracy of the DFT calculations for these types of systems, i.e., reactions of transition metal complex and metal-catalyzed olefin polymerization, has been extensively reviewed elsewhere.[60−62] Electronic configurations of molecular systems were described by restricted double-numerical basis sets with polarization functions for all atoms except for hydrogen. The $1s^2 2s^2 2p^6$ configuration on Ti atom was assigned to the core and treated by the frozen-core approximation. A geometry optimization was carried out using the Broydan−Fletcher−Goldfarb−Shanno[63−65] (BFGS) energy minimization algorithm for each molecule. The general gradient approximation (GGA) correction was applied to the energy calculation with the exchange functional of Becke[66] and the correlation functional of Perdew and Wang[67,68] after the energy was first calculated at the local density approximation (LDA) level.

The conductor-like screening model (COSMO)[69,70] implemented into DMol^3 was used for incorporating the solvent effect into the DFT calculation.[71] The dielectric constants for the solvents considered in this study, benzene (C_6H_6), chlorobenzene (C_6H_5Cl), and dichloromethylene (CH_2Cl_2), are 2.27, 5.62, and 9.08, respectively. The radius of each atom for construction of a cavity in the dielectric medium was put to be the value optimized from experimental results with the best accuracy (1.3 for H, 2.0 for C, 1.83 for N, 1.72 for O, 1.43 for Al, 2.10 for Si, 2.05 for Cl, and 1.47 for Ti in Å, respectively).[70]

The insertion of a monomer is performed by a stepwise decrease in the reaction coordinate, followed by full optimization of geometry with respect to all other degrees of freedom at each step, the so-called linear transit calculation. The reaction coordinate is defined as the distance between the C_α atom (i.e., the carbon which is directly attached to the titanium) and the carbon atom which is nearer to the C_α between two carbon atoms of ethylene monomer. The decrease in the reaction coordinate corresponds to an approach of a monomer toward the reactive site of the catalyst. By this stepwise insertion process described above, the reaction undergoes four distinctive states: π-complex, transition state, γ-agostic product, and β-agostic product. The π-complex is a local minimum on the energy profile during the monomer insertion, the transition state is a maximum point on the energy profile occurring in the reaction coordinate between the complex and the γ-agostic product, the γ-agostic product is a product directly obtained by ethylene insertion, and the β-agostic product is another conformer of product which is obtained by a rotation of $-CH_2CH_3$ group along the $C_\alpha-C_\beta$ bond followed by energy minimization. Although it has been theoretically reported that there exists an energy barrier for uptake of ethylene monomer in the IP model,[51,53] we are not able to find any significant energy barrier for uptake of ethylene monomer. We believe that the reason for the absence of activation energy for uptake of ethylene monomer is related to the pathway of ethylene approach, which is determined by the direction of ethylene approach relative to the spatial position of cationic catalyst and counterion. Indeed, the presence of energy barrier for ethylene uptake is highly dependent on the direction of ethylene approach.[51] Although there are some plausible other pathways of ethylene approach, we have focused on the effect of solvent polarity, and therefore only one pathway of ethylene approach is considered in this study.

The model of activated cationic catalyst (**CGC**$^+$), $[H_2SiCp(NCH_3)Ti-CH_3]^+$ (Cp = cyclopentadienyl), is the abbreviated form of activated Dow CGC,[72] which has been successfully used as a model catalyst for ethylene−styrene copolymerization in our previous DFT study.[39] A counterion was modeled by a chlorinated anionic methylalumoxane (**MAO**$^-$), whose structure has been adopted as a model of counterion for metallocene-based olefin polymerization by Fusco et al.[42] The structure of MAO has not been perfectly understood, although possible candidates for MAO structure have been proposed.[73,74] Therefore, we employed the Fusco's model as a **MAO**$^-$ counterion, which is one of the simplest model for MAO, while the model promises a considerable computational accuracy. The ionic pair (**IP**) of **CGC**$^+$ and **MAO**$^-$ was obtained by energy minimization and used as an active species for monomer insertion when the IP model is employed.

III. Results and Discussion

Ethylene Insertion in Gas State. The results of calculations without consideration of the solvent effect, i.e., in gas state, are presented in this section. Figure 1 shows the structures of **CGC**$^+$, **MAO**$^-$, and **IP**. The **IP** is energetically more stable than the completely separated state by 95.33 kcal/mol, which corresponds to a typical value of energy saved by an ionic pairing (∼100 kcal/mol) in gas state.[51]

The structures of π-complex (**C**), transition state (**T**), γ-agostic product (**P**γ), and β-agostic product (**P**β) during the first and the second ethylene insertions are presented in Figures 2 and 3, respectively, where the numbers, 1 and 2, behind the letters representing for the states denote the first and the second insertion, respectively, and the subscripts, cat and ip, denote the cationic model and the IP model, respectively. When overall characteristics of ethylene insertion following the two models are compared with each other, it reveals that

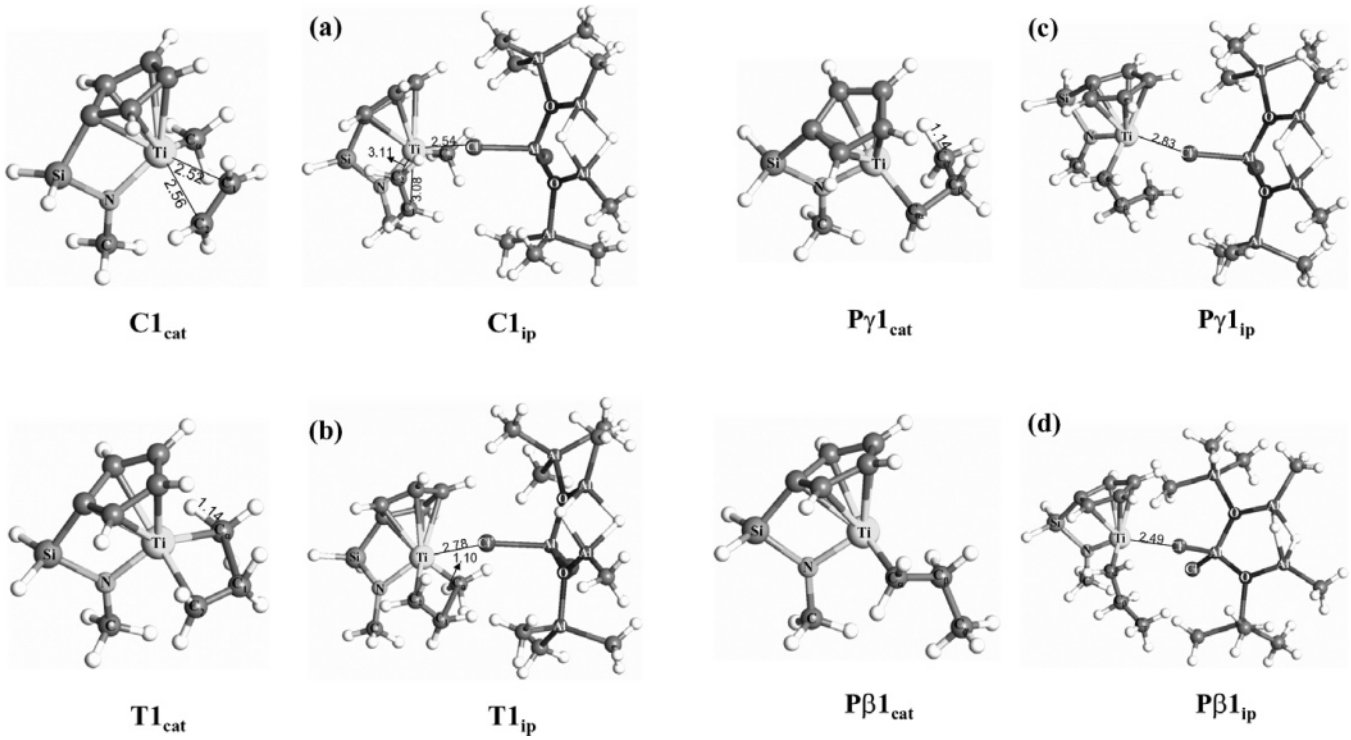

Figure 2. Structures at stationary points of (a) π-complex (**C**), (b) transition state (**T**), (c) γ-agostic product (**P**γ), and (d) β-agostic product (**P**β) for the first ethylene insertion using cationic (cat) and IP (ip) models.

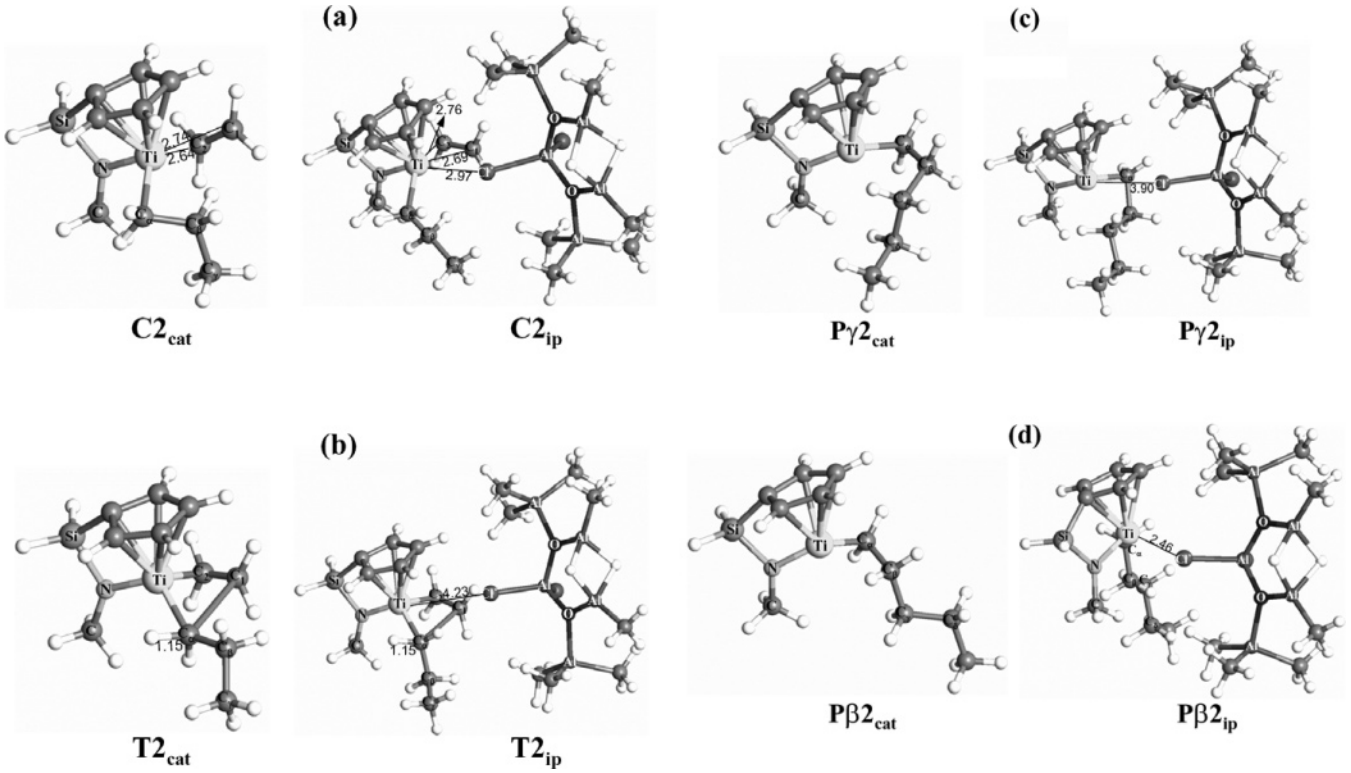

Figure 3. Structures at stationary points of (a) π-complex (**C**), (b) transition state (**T**), (c) γ-agostic product (**P**γ), and (d) β-agostic product (**P**β) for the second ethylene insertion using cationic (cat) and IP (ip) models.

two models predict common results as follows: (i) coordination of ethylene into the vacant site of Ti atom in π-complex, (ii) 4-centered ring structure in transition state, and (iii) stabilization of product via agostic interaction. This suggests that the cationic model, which has been conventionally used for mechanistic study on the metallocene-based polymerization, seems to provide a good insight for understanding the insertion mechanism. However, the model may not properly explain the mechanism of real situation, because the presence of counterion considerably changes the energetics of monomer insertion process, as shown in Figure 4.

Two important effects of the counterion on the energetics of monomer insertion are as follows: (i) First, the counterion changes the complexation energy (ΔE_{cx}), which is defined as the energy obtained by monomer

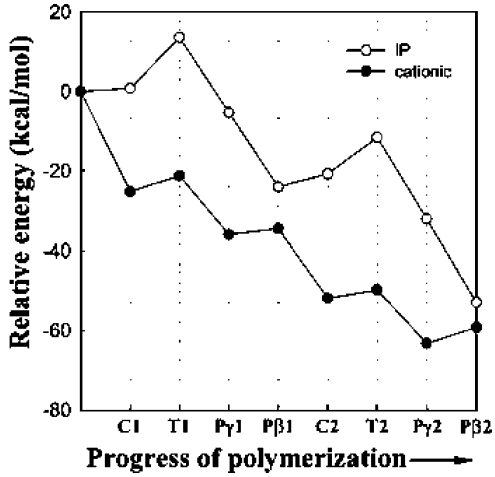

Figure 4. Energy profile for successive ethylene insertions using the cationic and IP models. The values of energies are relative to the energy of isolated free reactants, i.e., **CGC**$^+$ + **E** for the cationic model and **IP** + **E** for the IP model. Here, **E** represents ethylene monomer.

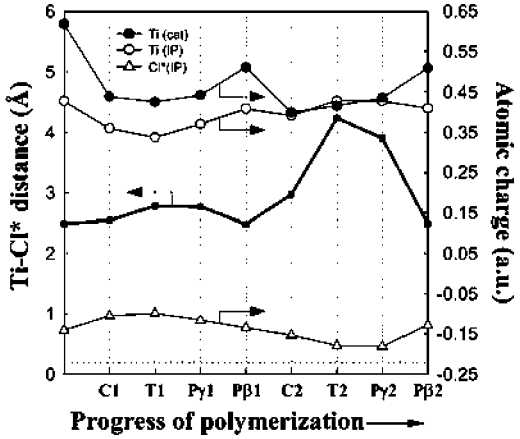

Figure 5. Profiles of Ti−Cl* distance and atomic charge of Ti and Cl* during successive ethylene insertions according to the cationic and IP models. The atomic charge of Cl in **MAO**$^-$ is also represented by dashed line at −0.22.

complexation, from exothermic to endothermic one. (ii) Second, the counterion increases the activation energy for monomer insertion (ΔE_a) which corresponds to the energy difference between π-complex and transition state. The reason for these was attributed mainly to a considerable separation of ionic pairs during monomer insertion, as explained by Lanza et al.[51] Our results are very consistent with their results, as shown in Figure 5, i.e., the Ti−Cl* distance increases temporarily during monomer insertion, where the Cl* represents a chlorine atom coordinated to Ti atom. The Ti−Cl* distance is reduced again as the β-agostic product is formed from the γ-agostic product by a positional rearrangement of the counterion (**MAO**$^-$), since the strong ionic pairing interaction is recovered, and thus the β-agostic product is considerably stabilized.

To understand more comprehensively the variation of the ionic pair interaction during ethylene insertion, we also calculated the atomic charge of Ti atom in both the cationic and the IP models and that of Cl* atom in the IP model at each stationary point using the Hirshfeld population analysis.[75] The results are listed in Table 1 and represented in Figure 5. For initiation (the first monomer insertion), the positive charge of Ti atom becomes less positive during monomer coordination in

Table 1. Charge (au) of Selected Atoms at Stationary Point during Insertion of Ethylene into CGC$^+$ (cationic) and IP (IP) in Gas State

	Ti (cationic)	Ti (IP)	Cl* (IP)
CGC$^+$	0.62		
MAO$^-$			−0.22
IP		0.43	−0.14
Cl	0.44	0.36	−0.11
Tl	0.43	0.34	−0.10
Pγ1	0.44	0.37	−0.12
Pβl	0.51	0.41	−0.14
C2	0.40	0.39	−0.15
T2	0.42	0.43	−0.18
Pγ2	0.44	0.43	−0.18
Pβ2	0.51	0.41	−0.13

both the cationic and the IP models, because an electron-rich ethylene monomer supplies electrons to the Ti atom during monomer coordination. The reduced Ti atomic charge becomes more positive again at the product as a new σ-bonding of Ti−C_α is formed with an old one being broken. The negative charge of Cl* atom counterbalances the positive charge of Ti atom at each state, i.e., the former becomes more/less negative while the latter becomes more/less positive, respectively.

For propagation (the second monomer insertion), the variation of charges of Ti and Cl* atoms in the IP model is different from that for initiation (the first monomer insertion), i.e., the charges for propagation become stronger (i.e., more positive for Ti and more negative for Cl*) during monomer coordination and then become weaker again at the final product. The reason for this is that the separation of ionic pair represented by the Ti−Cl* distance is larger in propagation than in initiation, as shown in Figure 5. The large separation of ionic pair reduces the electrons supplied by the counterion, and therefore, the atomic charge of Ti in the IP model becomes more positive (Figure 5).

Since the IP model becomes similar to the cationic model as the separation of ionic pair is larger, it is expected that the difference in the molecular structure between the two models is smaller for propagation than for initiation, as can be seen in Figures 2 and 3. For example, the Ti−C_1 distances of π-complex for propagation predicted by both models are very close to each other (2.69 Å in $\mathbf{C2_{ip}}$ vs 2.74 Å in $\mathbf{C2_{cat}}$ in Figure 3a), whereas the distances for initiation are largely different (3.08 Å in $\mathbf{C1_{ip}}$ vs 2.52 Å in $\mathbf{C1_{cat}}$ in Figure 2a).

Another interesting feature is that the relative stability between γ- and β-agostic products in the IP model is very different from that in the cationic model, i.e., the β-agostic product is much more stable than the γ-agostic product in the IP model, while the former is slightly less stable than the latter in the cationic model. In the IP model, the β-agostic structure is stabilized by recovery of strong ionic interaction between the two ionic species while the γ-agostic structure is unstable due to a considerable separation of the ionic pair. In the cationic model, however, the electron-deficient Ti atom of the γ-agostic structure has more chance to interact with hydrogen atoms in the growing alkyl chain than does the Ti atom of the β-agostic structure, and therefore the γ-agostic structure is more stabilized than the β-agostic structure, which has also been reported by Woo et al.[29] In short, the β-agostic product is a resting state in the IP model, whereas the γ-agostic product is a resting state in the cationic model for the CGC-based polymerization. The relative stability between the γ- and the β-agostic products, however, may be strongly af-

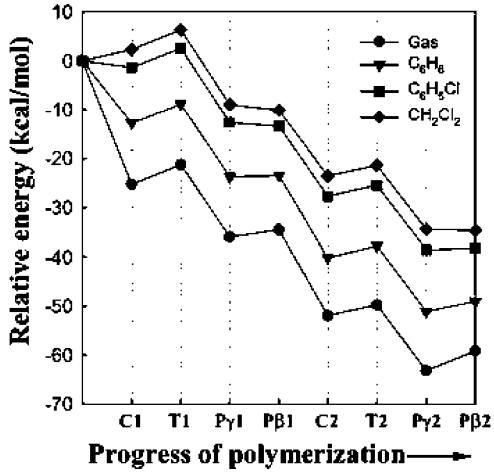

Figure 6. Effects of solvent polarity on the energy profile for successive ethylene insertions using the cationic model. The dielectric constants of solvents are 2.27, 5.62, and 9.08 for benzene (C_6H_6), chlorobenzene (C_6H_5Cl), and dichloromethylene (CH_2Cl_2), respectively.

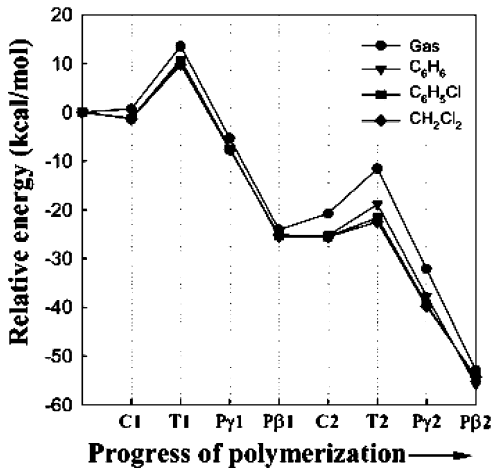

Figure 7. Effects of solvent polarity on the energy profile for successive ethylene insertions using the IP model. The dielectric constants for solvents are 2.27, 5.62, and 9.08 for benzene (C_6H_6), chlorobenzene (C_6H_5Cl), and dichloromethylene (CH_2Cl_2), respectively.

fected by the solvent polarity. More specifically, the resting state may change from the γ-agostic product to the β-agostic product in the cationic model, as the solvent polarity increases, which will be discussed in detail in the next section.

Ethylene Insertion in Solvent. The effect of solvent polarity on the energy profile of ethylene insertion using the cationic and the IP model are shown in Figures 6 and 7, respectively, and the energies at stationary points on the profiles are summarized in Table 2. To systematically analyze the effect of solvent polarity on the energetics of monomer insertion, we define four kinds of energies (ΔE) whose values are summarized in Table 3: (i) the ionic pairing energy (ΔE_{ip}), (ii) the complexation energy (ΔE_{cx}), (iii) the activation energy for ethylene insertion (ΔE_a), and (iv) the energy of β-agostic product relative to that of γ-agostic product ($\Delta E_{\beta\gamma}$).

Ionic Paring Energy. Figure 8 shows the effect of solvent polarity on the strength of ionic pairing, which is represented by the magnitude of the ionic pairing energy ($|\Delta E_{ip}|$). Here, the ionic pairing energy is defined by the energy of **IP** relative to the sum of energies of $\mathbf{MAO}^-$ and $\mathbf{CGC}^+$ for initiation (ΔE_{ip1}), and the energy of $\mathbf{P}\beta\mathbf{2}_{ip}$ relative to the sum of energies of $\mathbf{MAO}^-$ and more stable one between $\mathbf{P}\beta\mathbf{2}_{cat}$ and $\mathbf{P}\gamma\mathbf{2}_{cat}$ for propagation (ΔE_{ip2}). As shown in Figure 8, the ionic pairing strength decreases with increasing the solvent polarity, which is consistent with the results of previous theoretical studies.[48,51] Considering the fact that the activation energy in the cationic model is lower than that in the IP model, one may expect that the catalytic activity of polymerization increases with increasing the solvent polarity, because the separation of ionic pair increases with increasing the solvent polarity. Indeed, it is experimentally reported that the strength of ionic pairing between the cationic catalyst and its counterion is closely related to the catalytic activity of metallocene-based polymerization; i.e., the activity of polymerization is remarkably improved due to the polar solvent.[40,41,76−80] The increase of population of free cationic active species, which results from the increase of solvent polarity, explains the high activity observed.

A more interesting feature is that the ionic pairing strength is affected by the solvent polarity more strongly in initiation than in propagation, as shown in Figure 8. This is because the Ti atom of cationic catalyst is exposed to solvent medium more easily in initiation ($\mathbf{CGC}^+$) than in propagation ($\mathbf{P}\beta\mathbf{2}_{cat}$ or $\mathbf{P}\gamma\mathbf{2}_{cat}$), and as a result, the stability of $\mathbf{CGC}^+$ becomes more sensitive to solvent polarity than that of $\mathbf{P}\beta\mathbf{2}_{cat}$ or $\mathbf{P}\gamma\mathbf{2}_{cat}$.

Complexation Energy. The most noticeable difference between the cationic (Figure 6) and the IP (Figure 7) model is that the relative energies in the cationic model strongly depend on the solvent polarity while the energies in the IP model depend weakly on the solvent polarity. The primary reason for this is the difference between the two models in complexation energy (ΔE_{cx}), which is defined as the energy of π-complex relative to the sum of energies of a catalytic active species and a monomer. As shown in Figure 9, the complexation energy of cationic model decreases in magnitude with increasing the solvent polarity, while that of IP model does not change significantly with the solvent polarity. The dependence of the complexation energy on solvent polarity is more striking in initiation than in propagation. This is because the $\mathbf{CGC}^+$ has more open structure than $\mathbf{P}\beta\mathbf{2}_{cat}$ or $\mathbf{P}\gamma\mathbf{2}_{cat}$, and therefore it is more sensitive to the solvent polarity. It is interesting to note that the complexation of cationic model during initiation in dichloromethylene, the most polar solvent in our study ($\epsilon = 9.08$), is an endothermic process ($\Delta E_{cx} = 2.35$ kcal/mol), suggesting that in a highly polar solvent the interaction of the cationic catalyst with the solvent becomes stronger than that with monomer. This competing behavior in coordination with cationic active species between solvent and monomer has been observed in several experimental studies.[56,81] The competition usually results in considerable reduction of polymerization activity, which is consistent with our theoretical results, i.e., the exothermicity decreases with increasing the solvent polarity.

Unlike the cationic model, the complexation in the IP model changes from an endothermic process to an exothermic one, as the solvent polarity increases, as shown in Figure 9. This is because the destabilizing effect of counterion on π-complex in the IP model is screened by the polar solvent medium and thus the stability of the complex increases with increasing the solvent polarity. This is consistent with the previous study by Lanza et al.[51]

Table 2. Energies (kcal/mol) of Stationary Points Relative to the Energy of Isolated Free Reactants (CGC^+ + E for the Cationic Model and IP + E for the IP Model, Where E Represents Ethylene Monomer) during Insertion of Ethylene into CGC^+ (cationic) and IP (IP) in Gas or Solvent States[a]

	gas (1.00)		C_6H_6 (2.27)		C_6H_5Cl (5.62)		CH_2Cl_2 (9.08)	
	cationic	IP	cationic	IP	cationic	IP	cationic	IP
Cl	−25.23	0.71	−12.73	−1.21	−1.40	−1.29	2.35	−1.33
Tl	−21.23	13.56	−8.88	10.82	2.53	10.03	6.34	9.76
Pγ1	−36.00	−5.36	−23.67	−7.33	−12.60	−7.63	−8.94	−7.74
Pβl	−34.51	−24.09	−23.44	−25.62	−13.39	−25.23	−10.09	−25.12
C2	−51.91	−20.77	−40.14	−25.29	−27.64	−25.47	−23.54	−25.56
T2	−49.75	−11.55	−37.74	−18.88	−25.38	−21.62	−21.32	−22.45
Pγ2	−63.23	−32.12	−51.09	−37.68	−38.56	−39.28	−34.45	−39.82
Pβ2	−59.20	−52.97	−49.04	−55.80	−38.18	−54.61	−34.65	−54.25

[a] The dielectric constant (ϵ) of solvent is given in parentheses.

Table 3. Ionic Pairing Energy (ΔE_{ip}), Complexation Energy (ΔE_{cx}), Activation Energy for Ethylene Insertion (ΔE_a), and the Energy of β-agostic Product Relative to γ-Agostic Product ($\Delta E_{\beta\gamma}$) in kcal/mol during Insertion of Ethylene into CGC^+ (Cationic) and IP (IP) in Gas or Solvent States

	gas (1.00)		C_6H_6 (2.27)		C_6H_5Cl (5.62)		CH_2Cl_2 (9.08)	
	cationic	IP	cationic	IP	cationic	IP	cationic	IP
ΔE_{ipl}		−95.53		−51.97		−18.59		−8.21
ΔE_{cxl}	−25.23	−25.23	−25.23	−25.23	−25.23	−25.23	−25.23	−25.23
ΔE_{al}	4.00	12.85	3.85	12.03	3.93	11.32	3.99	11.09
$\Delta E_{\beta\gamma l}$	1.49	−18.74	0.23	−18.30	−0.79	−17.60	−1.15	−17.39
ΔE_{ip2}	-	−83.43	-	−53.92	-	−30.44	-	−23.24
ΔE_{cx2}	−17.40	3.33	−16.47	0.33	−14.25	−0.25	−13.45	−0.44
ΔE_{a2}	2.16	9.22	2.40	6.41	2.26	3.85	2.22	3.11
$\Delta E_{\beta\gamma 2}$	4.03	−20.85	2.05	−18.12	0.38	−15.34	−0.20	−14.44

[a] The dielectric constant (ϵ) of solvent is given in parentheses next to the chemical formula of each solvent and the definition of each energy difference (ΔE) is given as follows: $\Delta E_{ipl} = E(IP) - E(CGC^+) - E(MAO^-)$. $\Delta E_{cxl} = E(C1) - E(CGC^+) - E(E)$. $\Delta E_{al} = E(C1) - E(T1)$. $\Delta E_{\beta\gamma l} = E(P\beta 1) - E(P\gamma 1)$. $\Delta E_{ip2} = E(P\beta 2_{ip}) - E(P\beta 2_{cat}$ or $P\gamma 2_{cat})$. $\Delta E_{cx2} = E(C2) - E(P\beta 2$ or $P\gamma 2) - E(E)$. $\Delta E_{a2} = E(C2) - E(T2)$. $\Delta E_{\beta\gamma 2} = E(P\beta 2) - E(P\gamma 2)$. Here $E(A)$ represents the energy of structure A.

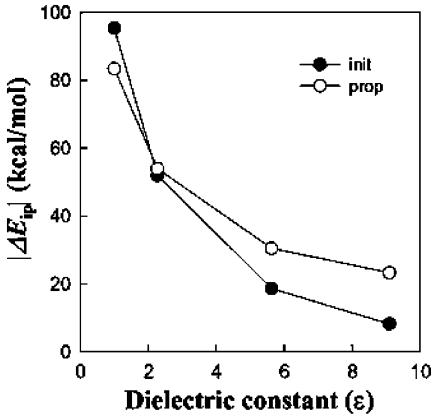

Figure 8. Effect of solvent polarity on the strength of ionic pairing ($|\Delta E_{ip}|$) for initiation and propagation according to the IP model. Here, the solvent polarity is represented with dielectric constant (ϵ).

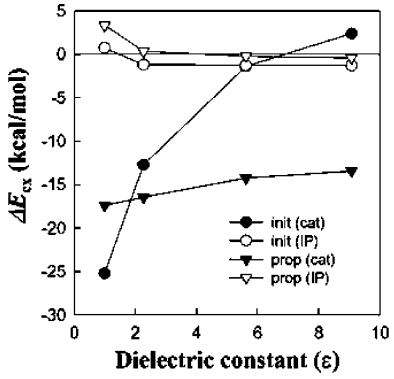

Figure 9. Effect of solvent polarity on the complexation energy (ΔE_{cx}) for initiation and propagation according to the cationic and IP models. Here, the solvent polarity is represented with dielectric constant (ϵ).

Activation Energy. Unlike the complexation energy, the activation energy (ΔE_a) is not dependent on the solvent polarity in the cationic model, as shown in Figure 10. This result provides very interesting information that if the solvent polarity is high enough to separate the ionic pair completely, the solvent with additionally higher polarity does not enhance further the activity of polymerization. The cationic model also shows that the activation energy for propagation is lower than that for initiation, which is consistent with an experimental result[30] where the initiation of polymerization is much slower than the propagation in metallocene-based polymerization.

The activation energy in the IP model, however, is dependent on the solvent polarity; i.e., it decreases with increasing the solvent polarity (Figure 10). This is because the transition state, which is unstable due to considerable separation of the ionic pair, can be stabilized by the polar solvent medium. As can be seen in Figure 10, the activation energy for propagation in the IP model decreases more rapidly than does the activation energy for initiation as the solvent polarity increases. This is because the separation of ionic pair at the transition state for propagation is larger than for initiation (see Figure 5). This reduction of activation energy with increasing solvent polarity is exactly consistent with experimental findings; i.e., the polymerization activity increases with increasing the solvent polarity.[76−80]

Relative stability of β- and γ-Agostic Products. Figure 11 shows that the energy of β-agostic product relative to that of γ-agostic product ($\Delta E_{\beta\gamma}$) in the cationic model changes from positive to negative as the solvent polarity increases. This means that the resting state of

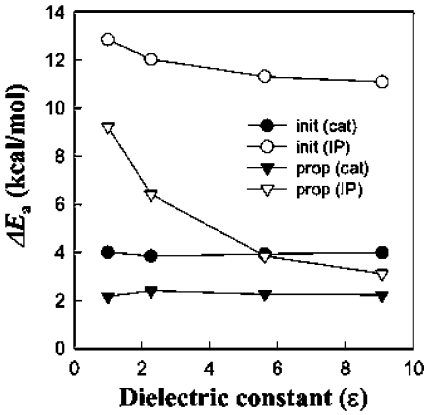

Figure 10. Effect of solvent polarity on the activation energy for monomer insertion (ΔE_a) for initiation and propagation according to the cationic and IP models. Here, the solvent polarity is represented with dielectric constant (ϵ).

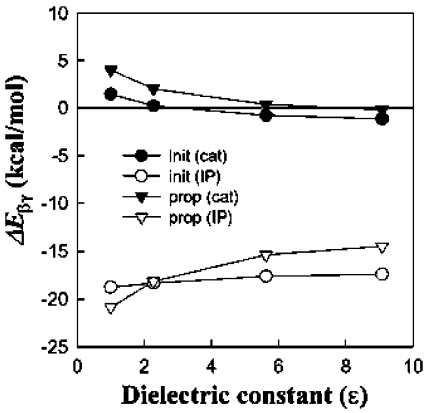

Figure 11. Effect of solvent polarity on the energy of the β-agostic product relative to that of γ-agostic product ($\Delta E_{\beta\gamma}$) for initiation and propagation according to the cationic and IP models. Here, the solvent polarity is represented with dielectric constant (ϵ).

catalytic active species for polymerization is a γ-agostic structure in low polar solvent while it is a β-agostic structure in higher polar solvent when the ionic pair is completely separated, i.e., in the cationic model. The change of relative stability of the two products depending upon the solvent polarity is closely related to the degree of exposure of the Ti atom to solvent medium, i.e., the β-agostic product, which is more open to the solvent medium than the γ-agostic product, exposes more the Ti atom to solvent medium than does the γ-agostic product, and as a result, the β-agostic product is more easily stabilized at higher polar solvents.

In the IP model, however, the β-agostic product is more stable than γ-agostic product regardless the solvent polarity, although the energy difference between the two products ($|\Delta E_{\beta\gamma}|$) decreases with increasing the solvent polarity, as shown in Figure 11. This is because the stabilizing effect of counterion due to recovery of strong ionic pairing interaction in the β-agostic product is much stronger than that in the γ-agostic product.

IV. Summary

From our calculation results, the relationship between the solvent polarity and the polymerization activity is established as follows: (i) when the ionic pair is not fully separated, i.e., in relatively low polar solvents, the activity of polymerization increases with increasing the solvent polarity, since the exothermicity of complexation increases (Figure 9) and the activation energy decreases with increasing the solvent polarity (Figure 10), and (ii) if the ionic pair is fully separated, i.e., in relatively high polar solvents, the activity of polymerization decreases with increasing the solvent polarity because the exothermicity of complexation decreases with increasing the solvent polarity (Figure 9) while the activation energy is not affected by the solvent polarity (Figure 10). According to this relationship, we can obtain a very useful information for identifying the real active species of the metallocene-based polymerization; i.e., if an experimental activity of polymerization increases as the solvent polarity increases, the catalytic active species of polymerization is ascribed to an ionic pair, but otherwise the catalytic active species is a free cation.

The most important features of molecular structure, which determine the dependence of enegetics on the solvent polarity, are summarized as (i) the degree of exposure of Ti atom to the solvent medium and (ii) the degree of separation of ionic pair during monomer insertion. The former influences mainly on the strength of ionic pairing, complexation energy and stability of resting state, while the latter has an effect on the activation energy for monomer insertion.

Acknowledgment. The authors thank the Korea Science and Engineering Foundation (KOSEF) through Hyperstructured Organic Materials Research Center (HOMRC) and Samsung General Chemicals Co. for their financial support.

Supporting Information Available: Tables of optimized Cartesian coordinates and absolute energies of all stationary points in gas state and in solution considered in this study. This material is available free of charge via the Internet at http://pubs.acs.org.

References and Notes

(1) Natta, G.; Dnausso, F.; Sianesi, D. *Makromol. Chem.* **1958**, *28*, 253.
(2) Kaminsky, W.; Külper, K.; Brintzinger, H. H.; Wild, F. R. W. P. *Angew. Chem.* **1985**, *97*, 507.
(3) Ishihara, N.; Seimiya, T.; Kuramono, M.; Uoi, M. *Polym. Prepr. Jpn.* **1986**, *35*, 240.
(4) Ewen, J. A.; Jones, R. L.; Razabi, A.; Ferrara, J. D. *J. Am. Chem. Soc.* **1988**, *110*, 6255.
(5) Scheirs, J.; Kaminsky, W. In *Metallocene-based Polyolefins: preparation, properties and technology*; John Wiley & Sons Ltd.: Chichester, U.K., 2000.
(6) Togni, A.; Halterman, R. L. In *Metallocenes: synthesis, reactivity, application*; Wiley-VCH: Weinheim, Germany, 1998.
(7) Long, N. J. In *Metallocenes: an introduction to sandwich complexes*; Blackwell Science: Malden, U.K., 1998.
(8) Novaro, O.; Blaisten-Barojas, E.; Clementi, E.; Giunchi, G.; Ruiz-Vizcaya, M. E. *J. Chem. Phys.* **1978**, *68*, 2337.
(9) Fuijimoto, H.; Yamasaki, T.; Mizutani, H.; Koga, N. *J. Am. Chem. Soc.* **1985**, *107*, 6157.
(10) Kawamura-Kuribayashi, H.; Koga, N.; Morakuma, K. *J. Am. Chem. Soc.* **1992**, *114*, 2359.
(11) Kawamura-Kuribayashi, H.; Koga, N.; Morakuma, K. *J. Am. Chem. Soc.* **1992**, *114*, 8687.
(12) Koga, N.; Yoshida, T.; Morokuma, K. *Organometallics* **1993**, *12*, 2777.
(13) Siegbahn, P. E. M. *Chem. Phys. Lett.* **1993**, *205*, 290.
(14) Weiss, H.; Ehrig, M.; Ahlrichs, R. *J. Am. Chem. Soc.* **1994**, *116*, 4919.
(15) Bierwagen, E. P.; Bercaw, J. E.; Goddard, W. A., III. *J. Am. Chem. Soc.* **1994**, *116*, 1481.
(16) Doremaele, G. H. J.; Meier, R. J.; Iarlori, S.; Buda, F. *J. Mol. Struct.* (*THEOCHEM*) **1996**, *363*, 269.
(17) Linnolahti, M.; Pakkanen, T. A. *Macromolecules* **2000**, *33*, 9205 and references reported therein.

(18) Lanza, G.; Fragala, I. L.; Marks, T. J. *Organometallics* **2001**, *20*, 4006.
(19) Amstrong, D. R.; Pekins, P. G.; Stewart, J. J. P. *J. Chem. Soc., Dalton Trans.* **1972**, 9172.
(20) Cassoux, P.; Crasnifer, F.; Labarre, J.-F. *J. Organomet. Chem.* **1979**, *165*, 303.
(21) McKinney, R. J. *J. Chem. Soc., Chem. Commun.* **1980**, 490.
(22) Balazs, A. C.; Johnson, K. H. *J. Chem. Phys.* **1982**, *77*, 3148.
(23) Shiga, A.; Kawamura, H.; Ebara, T.; Sasaki, T. *J. Organomet. Chem.* **1989**, *266*, 95.
(24) Prosenc, M.-H.; Janiak, C.; Brintzinger, H.-H. *Organometallics* **1992**, *11*, 4036.
(25) Coussens, B. B.; Buda, F.; Oevering, H.; Meier, R. J. *Organometallics* **1998**, *17*, 795.
(26) Woo, T. K.; Fan, L.; Ziegler, T. *Organometallics* **1994**, *13*, 2252.
(27) Fan, L.; Harrison, D.; Deng, L.; Woo, T. K.; Swerhone, D.; Ziegler, T. *Can. J. Chem.* **1995**, *73*, 989.
(28) Lohrenz, J. C. W.; Woo, T. K.; Fan, L.; Ziegler, T. *J. Organomet. Chem.* **1995**, *497*, 91.
(29) Woo, T. K.; Margl, P. M.; Lohrenz, J. C. W.; Blöchl, P. E.; Ziegler, T. *J. Am. Chem. Soc.* **1996**, *118*, 13021.
(30) Margl, P.; Deng, L.; Ziegler, T. *J. Am. Chem. Soc.* **1999**, *121*, 154.
(31) Lohrenz, J. C. W.; Bühl, M.; Weber, M.; Thiel, W. *J. Organomet. Chem.* **1999**, *592*, 11.
(32) Petitjean, L.; Pattou, D.; Ruiz-Lopez, M. −F. *J. Mol. Struct. (THEOCHEM)* **2001**, *541*, 227.
(33) Vanka, K.; Chan, M. S. W.; Pye, C. C.; Ziegler, T. *Macromol. Symp.* **2001**, *173*, 163.
(34) Margl, P.; Lohrenz, J. C. W.; Ziegler, T.; Blöchl, P. E. *J. Am. Chem. Soc.* **1996**, *118*, 4434.
(35) Sustmann, R.; Sicking, W.; Bandermann, F.; Ferenz, M. *Macromolecules* **1999**, *32*, 4204.
(36) Hyla-Kryspin, I.; Gleiter, R. *J. Mol. Catal. A: Chem.* **2000**, *160*, 115.
(37) Minieri, G.; Corradini, P.; Guerra, G.; Zambelli, A.; Cavallo, L. *Macromolecules* **2001**, *34*, 2459.
(38) Minieri, G.; Corradini, P.; Guerra, G.; Zambelli, A.; Cavallo, L. *Macromolecules* **2001**, *34*, 5379.
(39) Yang, S. H.; Jo, W. H.; Noh, S. K. *J. Chem. Phys.* **2003**, *119*, 1824.
(40) Fusco, R.; Longo, L.; Masi, F.; Garbassi, F. *Macromol. Rapid Commun.* **1997**, *18*, 433.
(41) Fusco, R.; Longo, L.; Masi, F.; Garbassi, F. *Macromolecules* **1997**, *30*, 7673.
(42) Fusco, R.; Longo, L.; Proto, A.; Masi, F.; Garbassi, F. *Macromol. Rapid Commun.* **1998**, *19*, 257.
(43) Bernardi, F.; Bottoni, A.; Miscione, G. P. *Oranometallics* **1998**, *17*, 16.
(44) Klesing, A.; Bettonville, S. *Phys. Chem. Chem. Phys.* **1999**, *1*, 2373.
(45) Nifant'ev, I. E.; Ustynyuk, L. Y.; Laikov, D. N. *Organometallics* **2001**, *20,* 5375.
(46) Chan, M. S. W.; Vanka, K.; Pye, C. C.; Ziegler, T. *Organometallics* **1999**, *18*, 4624.
(47) Chan, M. S. W.; Ziegler, T. *Organometallics* **2000**, *19*, 5182.
(48) Vanka, K.; Ziegler, T. *Organometallics* **2001**, *20*, 905.
(49) Lanza, G.; Fragalà, I. L.; Marks, T. J. *J. Am. Chem. Soc.* **1998**, *120*, 8257.
(50) Lanza, G.; Fragalà, I. L. *Top. Catal.* **1999**, *7*, 45.
(51) Lanza, G.; Fragalà, I. L.; Marks, T. J. *Organometallics* **2002**, *21*, 5594.
(52) Zakharov, I. I.; Zakharov, V. A. *Macromol. Theory Simul.* **2002**, *11*, 3.
(53) Xu, Z.; Vanka, K.; Ziegler, T. *Organometallics* **2004**, *23*, 104.
(54) Lanza, G.; Fragalà, I. L.; Marks, T. J. *J. Am. Chem. Soc.* **2000**, *122*, 12764.
(55) Forlini, F.; Fan, Z-. Q.; Tritto, I.; Locatelli, P.; Sacchi, M. C. *Macromol. Chem. Phys.* **1997**, *198*, 2397.
(56) Forlini, F.; Princi, E.; Tritto, I.; Sacchi, M. C.; Piemontesi, F. *Macromol. Chem. Phys.* **2002**, *203*, 645.
(57) Vanka, K.; Chan, M. S. W.; Pye, C. C.; Zieger, T. *Organometallics* **2000**, *19*, 1841.
(58) Yang, S. H.; Huh, J.; Yang, J. S.; Jo, W. H. *Macromolecules* **2004**, *37*, 5741.
(59) Delly, B. *J. Chem. Phys.* **1991**, *94*, 7245.
(60) Niu, S.; Hall, M. B.*Chem. Rev.* **2000**, *100*, 353.
(61) Rappé, A. K.; Skiff, W. M.; Casewit, C. J.*Chem. Rev.* **2000**, *100*, 1435.
(62) Angermund, K.; Fink, G.; Jensen, V. R.; Kleinschmidt, R.*Chem. Rev.* **2000**, *100*, 1457.
(63) Press, W. H.; Flannery, B. P.; Teukolsky, S. A.; Vetterling, W. T. In *Numerical Recipes, the Art of Scientific Computing*; Cambridge University Press: New York, 1986.
(64) Pulay, P. *J. Comput. Chem.* **1982**, *3*, 556.
(65) Csa'sza'r, P.; Pulay, P. *J. Mol. Struct.* **1984**, *114*, 31.
(66) Becke, A. D. *Phys. Rev. A* **1988**, *38*, 3098.
(67) Perdew, J. P.; Wang, Y. *Phys. Rev. B* **1992**, *45*, 13244.
(68) Perdew, J. P.; Chevary, J. A.; Vosko, S. H.; Jackson, K. A.; Pederson, M. R.; Singh, D. J.; Fiolhais, C. *Phys. Rev. B* **1992**, *46*, 6671.
(69) Klamt, A.; Schüürmann, G. *J. Chem. Soc., Perkin Trans. 2* **1993**, 799.
(70) Klamt, A.; Jonas, V.; Bürger, T.; Lohrenz, J. C. W. *J. Phys. Chem. A* **1998**, *102*, 5074.
(71) Andzelm, J.; Kölmel, C.; Klamt, A. *J. Chem. Phys.* **1995**, *103*, 9312.
(72) Stevens, J. C.; Timmers, F. J.; Wilson, D. R.; Schmidt, G. F.; Nickias, P. N.; Rosen, R. K.; Knight, G. W.; Lai, R. Eur. Patent. 416815, 1991; *Chem. Abstr.* **1991**, *115*, 93163.
(73) Zurek, E.; Woo, T. K.; Firman, T. K.; Ziegler, T. *Inorg. Chem.* **2001**, *40*, 361.
(74) Zurek, E.; Ziegler, T. *Organometallics* **2002**, *21*, 83.
(75) Hirshfeld, F. L. *Theor. Chim. Acta B* **1977**, *44*, 129.
(76) Longo, P.; Oliva, L.; Grassi, A.; Pellecchia, C. *Macromol. Chem.* **1989**, *190*, 2357.
(77) Herfert, N.; Fink, G. *Macromol. Chem.* **1992**, *193*, 773.
(78) Herfert, N.; Fink, G. *Macromol. Chem.*, *Macromol. Symp.* **1993**, *66*, 157.
(79) Vizzini, J. C.; Chien, C. W.; Babu, G. N.; Newmark, R. A. *J. Polym. Sci., Part A: Polym. Chem.* **1994**, *32*, 2049.
(80) Coevoet, D.; Cramail, H.; Deffieux, A. *Macromol. Chem. Phys.* **1996**, *197*, 855.
(81) Forlini, F.; Tritto, I.; Locatelli, P.; Sacchi, M. C.; Piemontesi, F. *Macromol. Chem. Phys.* **2000**, *201*, 401.

MA0481961